Research paper

Thermosensitive liposomes for triggered release of cytotoxic proteins

Maria B.C. de Matos[a], Nataliia Beztsinna[a], Christoph Heyder[b], Marcel H.A.M. Fens[a], Enrico Mastrobattista[a], Raymond M. Schiffelers[c], Gero Leneweit[b], Robbert J. Kok[a],*

[a] Department of Pharmaceutics, Utrecht Institute for Pharmaceutical Sciences (UIPS), Utrecht University, Utrecht, the Netherlands
[b] ABNOBA GmbH, Pforzheim, Germany
[c] Laboratory Clinical Chemistry & Haematology, University Medical Center Utrecht, the Netherlands

ARTICLE INFO

ABSTRACT

Lysolipid-containing thermosensitive liposomes (LTSL) are clinically-relevant drug nanocarriers which have been used to deliver small molecule cytostatics to tumors in combination with local hyperthermia (42 °C) to trigger local drug release. The objective of this study was to investigate the feasibility of LTSL for encapsulation and triggered release of macromolecular drugs such as plant-derived cytotoxins. As therapeutic protein we used Mistletoe lectin-1 (ML1) - a ribosome-inactivating protein with potent cytotoxic activity in tumor cells.

Model macromolecules (dextrans, albumin) and ML1 were encapsulated in small unilamellar LTSL with varying lipid compositions by the thin film hydration method and extrusion. LTSLs showed molecular weight dependent heat-triggered release of the loaded cargo. The most promising composition, ML1 formulated in LTSL composed of 86:10:4 %mol DPPC:MSPC:DSPE-PEG$_{2000}$, was further studied for bioactivity against murine CT26 colon carcinoma cells. Confocal live-cell imaging showed uptake of released ML1 after mild hyperthermia at 42 °C, subsequently leading to potent cytotoxicity by LTSL-ML1. Our study shows that LTSL in combination with localized hyperthermia hold promise as local tumor delivery strategy for macromolecular cytotoxins.

1. Introduction

Over the past decades, nanomedicines have gained attention as targeted formulations for cancer therapy. Due to the leakiness of tumor blood vessels and impaired lymphatic system, long-circulating nanoparticles such as PEGylated liposomes extravasate and accumulate in tumors, a phenomenon described as the enhanced permeability and retention (EPR) effect [1]. A more recent development in the nanomedicine field are nanocarrier systems that can be triggered with an external stimulus like heat, light or ultrasound [2–7]. Triggerable nanocarrier systems are especially interesting for cancer therapy, as they allow local controlled drug release thus limiting the toxicity of the payload to normal tissues and intensifying the peak concentrations of the active compounds within the tumor [2,8–14]. Lysolipid containing thermosensitive liposomes (LTSL), like the ThermoDox® formulation, are a well-studied example. They have shown superior activity in progression-free survival as well as in overall survival in clinical trials [14].

When thermosensitive liposomes are exposed to heating, the lipid bilayer undergoes a melting phase transition from a gel to a liquid-crystalline phase, allowing a rapid increase in bilayer permeability and thus rapid release of small solutes. The exact temperature and broadness of the phase transition depend on the lipid composition and can be adjusted to clinically relevant mild-hyperthermia temperatures (39–43 °C) [2,12,15]. The increased bilayer permeability in ThermoDox®, compared with traditional thermosensitive liposomes, relies on the inclusion of the lysolipid 1-stearoyl-2-hydroxy-sn-glycero-3-phosphatidylcholine (MSPC or Lyso-PC) in a 1,2-dipalmitoyl-sn-glycero-3-phosphocholine (DPPC) and N-(carbonyl-methoxypolyethyleneglycol$_{2000}$)- 1,2-distearoyl-sn-glycero-3-phosphoethanolamine (mPEG$_{2000}$-DSPE) (10:86:4 molar ratio, respectively).

Up to now, thermosensitive liposomes have been mainly used for the encapsulation and triggered release of small molecule drugs like doxorubicin, cisplatin, taxol, melphalan, methotrexate, plumbagin, dacarbazine, mitomycin C, and paclitaxel [7,8,10,15–21]. Encapsulation of macromolecular drugs in LTSL may seem counterintuitive, as they may not be released from this type of nanocarriers upon changes in bilayer fluidity. Still, a few examples exist of LTSL loaded with macromolecules such as TNFα, exist. They report successful, though incomplete, release under mild hyperthermia [22,23]. We now report on LTSL-encapsulation of mistletoe lectin I (ML1), a potent cytotoxin that

is one of the main active components of *Viscum album* extracts used as an adjuvant in complementary medicine practices [24,25]. Combining LTSL/intratumoral triggered release with the potent cytotoxins can be promising for cancer treatment. Upon prolonged circulation and the potential of EPR uptake in the tumor parenchyma, the site of drug release from PEGylated LTSL depends on the timing between intravascular administration and triggered release. We aim for a deliberate waiting time of several hours between liposome administration and local (tumor) hyperthermia, thus aiming for extravascular intratumoral release which seems most appropriate for high-MW cargo.

Mistletoe lectin-I belongs to the class of plant derived ribosome inactivating proteins (of class II, RIP-II) which interfere in protein biosynthesis via their rRNA N-glycosidase activity. The cytotoxic activity has been ascribed to the A-chain, which is linked to the B-chain that binds to cell-surface expressed receptors on target cells and hence mediates internalization of the RIP-II protein [26–30]. ML1 displays very fast binding to sugar residues on the cell membrane and its endocytosis involves both clathrin-dependent and -independent pathways [31]. ML1 is then transported from early endocytic vesicles to Golgi network and in a retrograde way to the endoplasmic reticulum, where it inactivates the ribosomes, leading to the disruption of protein biosynthesis, and eventually cell death [26–30]. RIP-II glycoproteins and plant extracts containing these cytotoxins have also been associated with activation of the immune system, which serves as alternative mechanism of anticancer activity. [29,30].

Intratumoral delivery and on-site release via thermosensitive liposomes seems an attractive strategy to improve the therapeutic window of ML1 and similar cytotoxins. We therefore explored the encapsulation and hyperthermia triggered release of model macromolecules and ML1. Our final obtained formulation showed good storage stability and stability at conditions reflecting the circulation of liposomes in the blood stream, while triggered release was induced by mild hyperthermia of 42 °C. Functional bioactivity of ML1 released from hyperthermia-triggered LTSL was studied by live-cell confocal fluorescence imaging and cell viability assays, demonstrating uptake of released ML1 by tumor cells and subsequent cytotoxic activity.

2. Materials and methods

2.1. Chemicals

The phospholipids 1,2-dipalmitoyl-sn-glycero-3-phosphocholine (DPPC), and 1,2- distearoyl-sn-glycero-3-phosphoethanolamine-N-PEG$_{2000}$ (DSPE- PEG$_{2000}$) were purchased from Lipoid (Ludwigshafen, Germany). 1-stearoyl-2-hydroxy-sn-glycero-3-phosphocholine (MSPC) were purchased from Avanti Polar Lipid Inc (Alabaster, USA). FITC-labeled BSA and Dextran 4 kDa were obtained from Sigma Aldrich (Zwijndrecht, Netherlands), while FITC-labeled Dextran 10 kDa was purchased from Nanocs (New York, USA). Isolated Mistletoe Lectin-1 and control standard for ELISA (4.5 μg/ml) were isolated according to the protocols provided by Eifler et al. [32]. Anti-ML-A-5F5, and Anti-ML-A-5H8-POD monoclonal antibodies with specificity to ML1 A-chain were both obtained from SIFIN (Berlin, Germany). CellTiter 96® AQueous One Solution Cell Proliferation Assay (MTS) was provided by Promega (Leiden, The Netherlands). The lipophilic fluorescent dye 3,3′-dioctadecyloxacarbocyanine perchlorate ('DiO'; DiO-C18(3)) and Alexa Fluor® 647 succinimidyl ester (Alexa 647 NHS) were purchased from Invitrogen (Landsmeer, The Netherlands). Chemicals used in cell culture (RPMI, FBS, tripsin, PBS) were purchased from Sigma-Aldrich (Zwijndrecht, Netherlands). The murine colon carcinoma cell line CT26 was obtained from American Type Culture Collection (ATCC, Wesel, Germany).

2.2. Mistletoe lectin-1 isolation and characterization

For ML1 isolation, mistletoe plant material was harvested in June from ash tree (*Fraxinus excelsior* L.) and extraction was performed at

ABNOBA GmbH by affinity chromatography as described previously [32], using the affinity of ML1 for D-galactose. After purification, ML1 was characterized by FPLC using a Mono S cation exchange column (Pharmacia/GE Healthcare, Uppsala, Sweden) and a0.6 M NaCl salt gradient in 0.015 M citrate buffer (pH 4.0) at a detection wavelength of 280 nm. For chromatograms, see [31].

ML1 was exposed to high temperatures and sheer-stress both during encapsulation/extrusion and upon hyperthermia-triggered release from liposomes. Therefore, we evaluated the bioactivity of ML1 against CT26 cells (10,000 cells/well, see Uptake and Bioactivity section for further details on cell culture conditions) after different heat treatments: (1) after exposure to 42 °C in an Eppendorf thermoshaker, (2) after exposure to 55 °C and 15x extrusion through 100 nm pore size polycarbonate membrane (ca. 15 min), and (3) after the sequential exposure to 55 °C extrusion and 42 °C (ca. 1 h 15 min in total). After 48 h incubation, MTS conversion was measured and the dose–response curves and IC$_{50}$ where analysed and compared to the ML1 untreated control.

2.2.1. SDS-PAGE

The identification of molecular weight of native ML1 was performed by non-reducing SDS-PAGE (50 min at 165 V). ML1 was pretreated with saturated iodoacetamide solution (1:2) for 30 min at room temperature to prevent autolytic cleavage of the disulfide bond which covalently links A and B chains. NuPAGE Bis-Tris Gels (12% polyacrylamide, Novex, Life Technologies) were stained using Coomassie blue.

2.2.2. Quantification by NanoDrop and ELISA

ML-1 was quantified by UV/Vis using NanoDrop ND-1000 (Thermo Fisher Scientific) at 280 nm using an extinction coefficient of 104,850 M^{-1}cm^{-1}. ML1 was also experimentally quantified by sandwich ELISA. Briefly, the wells of a 96 well plate were coated with primary antibodies (9 μg/mL, bicarbonate buffer, Anti-ML-A-5F5, 100 μL per well) by incubating at room temperature for 30 min. Following three washes with PBS–Tween (each 100 μL), the plate was incubated for 30 min with ML1 samples and standards (each 100 μL/well). The plate was again washed with PBS-Tween buffer (3 × 100 μL/well). Then wells were coated with the secondary peroxidase antibodies Anti-ML-A-5H8 (10 μg/mL, 100 μL/well) and incubated at room temperature for 30 min. After PBS-Tween buffer wash, the plate was incubated with 100 μL/well of TBM substrate. Finally, the reaction was stopped by addition of 100 μL/well 1 M sulfuric acid. The yellow colored reaction product was detected at 450 nm with the spectrometric plate reader.

2.2.3. ML1 labeling with AlexaFluor 647

ML1 conjugation to Alexa Fluor 647 (AF647) succinimidyl ester was performed in accordance to manufacturer's protocol. In brief, 250 μL of 0.02 M bicarbonate buffer pH 8.3 was added to 2 mL of ML1 5.6 mg/mL (12 mg, 0.2 μmol). The diluted protein was reacted with AF647 dye (5:1 dye:protein mol/mol; 100 μg/in 20 μL DMSO)20 5:1 dye: ML1 ratio) The mixture was stirred at room temperature for 1 h and purified by size exclusion chromatography (PD10 disposable columns, GE Healthcare Life Sciences). Purified AF647-ML1 was characterized by analytical size-exclusion chromatography on a Bio Sep 3000 column, 20 min, PBS 1 mL/min). The labeled ML1 was kept protected from the light at 4 °C until further use.

2.3. Preparation of LTSL

Liposomes with different lipid compositions (lipid molar ratio of DPPC/MSPC/DSPE-PEG$_{2000}$ for LTSL5: 91/5/4; for LTSL10: 86/10/4; for LTSL15: 81/15/4) were prepared by the lipid film and extrusion. Typically, 250 μmol of lipids (and DiO at 0.5% mol of total lipid, for lipid bilayer labeling) were dissolved in 1:1 chloroform/methanol; and the organic solvents were evaporated for 20 min in the rotavapor (thin-film) at 60 °C. The films were kept for 1 h in nitrogen stream and later hydrated at 50 °C with HBS (10 mM HEPES buffer with 0.9% w/v NaCl),

with or without macromolecules dissolved. Lipid film formation and reconstitution, typically in 5 mL of buffer, resulted in a final lipid concentration of 50 mM. Extrusion was done 15 times over 400 and 100 nm pore-size polycarbonate filters at 50 °C. The lipid concentration of LTSL encapsulating ML1 was 50 mM, but the batch size was smaller (1 mL, 50 μmoL total lipid). When applicable, liposomes were separated from non-encapsulated cargo by ultracentrifugation (Beckmann ultracentrifuge, 3x, 55000 rpm 60 min 4 °C), and stored at 4 °C.

2.4. Characterization of LTSL

2.4.1. Size, polydispersity index, zeta potential and phosphate yield

The hydrodynamic diameter and polydispersity index of all liposomes were measured by dynamic light scattering using a Malvern ALV/CGS-3 multiangle goniometer with He − Ne laser source ($\lambda = 632.8$ nm, 22 mW output power) under an angle of 90° (ALV, Langen, Germany). The zeta-potential of the liposomes was measured using laser Doppler electrophoresis on a Zetasizer Nano-Z (Malvern Instruments) with samples dispersed in 10 mM HEPES buffer pH 7.4 (with no additional salts added). The total phosphate content of the liposome formulations was determined according to the method of Rouser et al. [33] with sodium biphosphate as a standard after destruction of the phospholipids with perchloric acid and heating at 180 °C. The blue coloured reaction product was detected at 797 nm with the spectrometric plate reader.

2.4.2. Encapsulation efficiency

An aliquot of 50 μL of liposome suspension was diluted in 450 μL of HBS, to which TritonX-100 0.1% v/v was added to destroy the liposomes. The amount of encapsulated compound was determined by fluorometry (in the case of model compounds) or by ELISA (in the case of ML1, see above) and calculated as follows:

$$EE\% = \frac{total\ amount\ of\ payload\ in\ liposomes}{initial\ amount\ of\ payload} \times 100 \tag{1}$$

2.4.3. Storage stability

Storage stability of LTSL at 4 °C was extrapolated from size/PDI variations (using the same methods as presented above) and drug retention capacity over a period of 3 weeks. At each time point, an aliquot of liposomes suspension was separated from the free drug by means of ultrafiltration (Vivaspin 500 MWCO 300 000 Da). The flow-through was analyzed by fluorometry (in the case of model compounds) or by ELISA (in the case of ML1; see below) and calculated as:

$$Drug\ retention\ [\%] = \frac{payload_t}{payload_i} \times 100 \tag{2}$$

where $payload_t$ is mass of compound found outside (in the flow-through) the LTSL at a certain time point, $payload_i$ is the mass found inside the liposomes in the beginning of the experiment.

2.4.4. Differential scanning calorimetry

DSC was carried out to a have a better insight about the thermal properties of the LTSLs, for further studies of thermal-induced release, live-imaging with mild hyperthermia in cells. DSC measurements (DSC Discovery, TA Instruments, New Castle, USA) were carried out in duplicate, starting by equilibrating the samples and reference at 25 °C for 5 min and then ramping from 25 °C to 55 °C, at 1 °C/min.

2.5. Release experiments

2.5.1. Temperature-dependent release

LTSL suspensions were incubated in preconditioned HBS (22, 37, 40 and 42 °C) under stirring (300 rpm) in a thermomixer. After incubation at the designated temperature for 15 min, the samples were immediately transferred to an ice bath to avoid further leakage. LTSL

samples kept at 4 °C were considered as a blank and LTSL samples destroyed with TritonX-100 were considered as the 100% release. Separation of released cargo from LTSL was done by ultrafiltration with Vivaspin columns and the flow-through was analyzed by fluorometry (model compounds) or ELISA (ML1) as described above.

2.5.2. Time-dependent release

Time-dependent release profiles of LTSLs were performed at 37 °C and 42 °C. LTSL suspensions were diluted in pre-heated HBS during fixed intervals (5, 10, 15, 30 min) under stirring (300 rpm) in a thermomixer. LTSL samples kept at 4 °C were considered as a blank and LTSL samples destroyed with TritonX-100 were considered as the 100% release. Separation of released cargo from LTSL by Vivaspin ultrafiltration and analysis of labeled macromolecules (fluorometry) or ML1 (ELISA) was done as described above.

In all release experiments, the percent release of the compounds was quantified by using the equation:

$$Release\% = \frac{payload_t - payload_0}{payload_{triton} - payload_0} \times 100 \tag{3}$$

where $payload_t$ is mass determined of compound at a certain time point or fixed temperature, $payload_0$ is the mass found outside the liposomes in the beginning of the experiment (typically zero) and $payload_{triton}$ is total mass found after liposomes were treated with Triton X-100.

2.6. Uptake and bioactivity of LTSL-ML1 under normothermia and mild hyperthermia conditions

The functional activity of ML1 was studied using CT26 colon carcinoma cells, which are sensitive to ML1 at low nM ranges [31]. CT26 cells were culture in RPMI supplemented with 10% FBS, at 37 °C in a 5% CO_2 and humidified atmosphere. Two different heat treatment schedules were used to explore uptake and bioactivity of ML1. While the first approach was used to demonstrate the functional activity of ML1 that was first released from LTSL, the second approach simulated the hyperthermia treatment of tumor nodules in which ML1 is released from liposomes after intratumoral accumulation by EPR.

For all the experiments and for both experimental setups (see experimental details below), CT26 colon carcinoma cells were first seeded in 96-well plates (10,000 cells/well) 24 h prior to the experiment. For live cell confocal imaging microscopy experiments, DiO' labeled liposomes loaded with AF647-labeled ML1 were used and nuclei of CT26 cells were prestained with Hoechst 33342.

Non-labeled ML1 and liposomes were used for cell-viability experiments and nuclei were not prestained with Hoechst 33342.

2.6.1. Heat-treatment schedules and ML1 uptake and bioactivity for setup 1

LTSL10-DiO' loaded with AF-647-labeled ML1 and control formulations as specified in the result section were diluted in OptiMEM (final concentrations 10 μg/mL AF647-ML-1 and 8 mM total lipid) and incubated for 1 h at 42 °C (hyperthermia triggered media) or for 1 h at 37 °C (normothermic media) in a pre-thermostated Eppendorf thermoshaker. The incubated media were then transferred without any separation/purification step onto CT26 cells kept at 37 °C and previously stained with Hoechst 33342. Live cell images were taken for 4 h in a fluorescent confocal Yokogawa Cell Voyager CV7000s microscope (Tokyo, Japan).

To determine cytotoxic activity, ML1 formulated in LTSL10 or ML1 loaded in control PEG liposomes were diluted in OptiMEM to final concentration ranges of 0.3–10 μg/mL ML-1 (5–167 nM); corresponding to 0.2–8 mM total lipid. Spiked media were incubated for 1 h at 42 °C (hyperthermia triggered media) or for 1 h at 37 °C (normothermic control media) in a pre-thermostated Eppendorf thermoshaker. The preconditioned media were then transferred without any separation/purification step onto CT26 cells that were subsequently cultured at 37 °C under standard culture conditions (see above) for 4 h. After the

4 h contact period, the drug containing media were refreshed with drug-free culture medium and cells were cultured for an additional 44 h at 37 °C in the incubator. ML1 bioactivity was assessed by its effect on cell survival as assessed by MTS conversion (CellTiter 96® AQueous One Solution Cell Proliferation Assay) at 490 nm in a well plate reader. OptiMEM spiked with ML1, empty LTSL10, and conventional liposomes (NTL, non-thermosensitive liposomes) loaded with ML1 were submitted to the same protocol and used as controls. IC_{50} values of each treatment were calculated by non-linear curve fitting using GraphPad Prism software, assuming sigmoidal dose-response curves for all data sets including experiments that did not reach 100% cell killing.

2.6.2. Heat-treatment schedules and ML1 bioactivity for setup 2

The second heat treatment schedule involved mild hyperthermia of CT26 cells in the presence of ML1-loaded LTSL treatment (42 °C for 1 h; versus normothermic conditions of 37 °C for 1 h), which was either effectuated directly in the microscope plate chamber (live cell imaging) or by incubating cells in a water bath (cell viability experiments). For live cell imaging, the CV7000s microscope plate chamber was heated to the desired temperature (37 °C or 42 °C). OptiMEM was spiked with AF647-labeled ML1 formulated in DiO'-labeled LTSL (final concentration final concentrations 10 µg/mL AF647-ML-1 and 6 mM total lipid), after which media were pipetted onto the cells and well plates were transferred into the microscope plate chamber. Cellular uptake of ML1 was imaged by live-cell confocal microscopy for 1 h at the stated temperatures. Confocal images were analyzed with Columbus® image analysis software (PerkinElmer) using automated segmentation protocols for nuclei and cytoplasm detection and build-in functionalities for average fluorescence intensity determination.

In a parallel experiment, OptiMEM was spiked with various concentrations of non-labeled ML1 formulated in LTSL10 (final concentration of ML1: 0.22–10 µg/mL or 4–167 nM; corresponding total lipid concentration range 0.2–6 mM). Drug-spiked media were transferred onto CT26 cells after which the well plates were tightly sealed with parafilm and subsequently incubated for 1 h at 42 °C or for 1 h at 37 °C in a water bath, previously heated to the desired temperatures. Next, after refreshing the media with drug-free culture medium, CT26 cells were cultured for an additional 47 h at 37 °C in the incubator. Cytotoxic effects of ML1 were determined by MTS assay and non-linear curve fitting as described above.

2.7. Statistical analysis

Data are presented as average with standard deviation. Statistical differences between groups were computed using GraphPad Prism7 with 95% confidence one-way ANOVA using Tukey's multicomparison test.

3. Results and discussion

3.1. Characterization of mistletoe lectin-1

ML1 was isolated from freshly harvested mistletoe plant material as described in the materials and methods section and was characterized by SDS-PAGE, ELISA and bioactivity (MTS) as presented in the supporting information (Supplementary Fig. SI-1). As expected from its structure (UniProtKB-P81446, EC 3.2.2.22; MW 62628 Da), ML1 migrated in SDS-PAGE around 60 kDa; no bands were observed at higher molecular weights indicating that there were no multimers in the isolated product. In addition, no bands were observed in the 20–30 kDa range, meaning that the ML1 was intact and had not dissociated into the two (A and B) chains. The concentration of the ML1 stock solution was quantified by two different methods, UV-absorbance at 280 nm and an anti-ML1 sandwich ELISA, which both yielded similar values (5.6 and

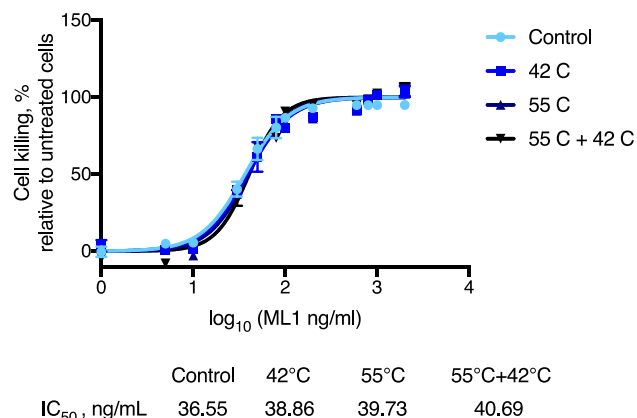| IC_{50}, ng/mL	Control	42°C	55°C	55°C+42°C
	36.55	38.86	39.73	40.69

Fig. 1. Bioactivity of ML1 exposed to different heat conditions versus CT26 colon carcinoma cells after 48 h incubation: light blue line control (untreated) ML1; royal blue 42 °C line represents the effect of mild hyperthermia; dark blue 55 °C line represents the effect of extrusion temperature and shear forces; black 55 °C + 42 °C line represents the combination effect of extrusion and mild hyerthermia. (For interpretation of the references to colour in this figure legend, the reader is referred to the web version of this article.)

4.6 mg/mL for UV absorbance and ELISA respectively). For the remaining experiments, we used the ELISA method in view of its higher sensitivity.

Since ML1 is exposed to sheer-stress and hyperthermia both during encapsulation/extrusion and upon hyperthermia-triggered release from liposomes, we evaluated the bioactivity of ML1 after different heat treatments. Neither treatment diminished the bioactivity of ML1, i.e. the effect of extrusion at 55 °C, mild-hyperthermia at 42 °C for 1 h , and their combination (55 °C + 42 °C) did not result in altered dose-response curves of ML1 versus CT26 colon carcinoma cells (Fig. 1). Collectively, the characterization data confirmed the identity and bioactivity of the isolated ML1 in line with previously reported studies [31].

3.2. Characterization of LTSL: size, polydispersity index, encapsulation efficiency, thermal properties and shelf-life

Table 1 shows characterization data of LTSL with different lipid compositions that had been loaded by the film hydration method with fluorescein-labeled macromolecules ranging in MW from 4kD-67 kDa, with diverse structures (dextrans, albumin and ML1). The size (111–146 nm) and polydispersity (0.04–0.15) of LTSL were similar between loaded and non-loaded formulations, irrespectively of the loaded macromolecule (Table 1). Similar encapsulation efficiencies were found for all samples (6–10%), i.e. no specific trend was observed towards the lipid composition and/or the loaded molecule.

Ultracentrifugation was used to purify the LTSL from unencapsulated payload, after which the collected pellet was carefully resuspended in HBS buffer. We validated that such a procedure did not adversely affect colloidal stability and retention of loaded ML1 by analyzing size, phospholipid recovery and ML1 retention after three consecutive cycles of ultracentrifugation and resuspension (Supplementary Fig. SI-2). No changes in size of liposomes and ML1/lipid content were observed.

The capability of LTSL to release their loaded cargo upon mild hyperthermia is attributed to phase transitions of the bilayer during the melting of DPPC around 40–42 °C. The transition temperature was not affected by the presence of encapsulated macromolecules (Table 2). Minor differences were observed in the transition enthalpy (ca. 0.15 J/g) between dextran loaded and BSA loaded LTSL, and our hypothesis is that protein hydrophobic domains of BSA may interact with the lipid

Table 1
Initial physicochemical features of all the LTSL formulations prepared with varying mixtures of DPPC/MSPC/DSPE-PEG$_{2000}$. LTSL5: 91/5/4 %mol; LTSL10: 86/10/4 %mol; LTSL15: 81/15/4 %mol. Average $\pm$ standard deviation of 2 independent samples; Loading = μg cargo/ mmol lipid; n.a. = non-applicable.

Formulation		Size (nm)	PDI	Zeta potential (mV)	Encapsulation efficiency (%)	Loading content, (μg/mmol lipid)
Control	LTSL5	132 ± 0	0.08 ± 0.00	−13.6 ± 0.8	n.a.	n.a.
	LTSL10	136 ± 2	0.04 ± 0.01	−8.5 ± 0.3	n.a.	n.a.
	LTSL15	146 ± 3	0.05 ± 0.05	−12.0 ± 0.4	n.a.	n.a.
4 kDa dextran	LTSL5	115 ± 0	0.07 ± 0.03	−8.7 ± 0.1	8.6 ± 0.1	2.4 ± 0.2
	LTSL10	134 ± 4	0.03 ± 0.00	−2.3 ± 0.4	7.9 ± 0.3	2.1 ± 0.1
	LTSL15	120 ± 1	0.15 ± 0.02	−8.1 ± 1.1	9.3 ± 0.6	3.4 ± 0.1
10 kDa dextran	LTSL5	111 ± 0	0.05 ± 0.04	−8.5 ± 0.3	7.8 ± 0.6	2.0 ± 0.3
	LTSL10	141 ± 9	0.10 ± 0.09	−12.8 ± 0.1	10.1 ± 0.1	3.0 ± 0.1
	LTSL15	119 ± 1	0.15 ± 0.04	−8.5 ± 0.3	6.2 ± 0.1	2.1 ± 0.4
60 kDa ML1	LTSL5	137 ± 3	0.10 ± 0.01	−11.3 ± 0.1	6.1 ± 0.5	1.6 ± 0.2
	LTSL10	133 ± 7	0.06 ± 0.01	−12.9 ± 0.2	8.8 ± 1.3	2.4 ± 0.2
	LTSL15	193 ± 2	0.16 ± 0.06	−10.7 ± 0.6	4.3 ± 2.1	1.4 ± 0.5
67 kDa BSA	LTSL5	131 ± 4	0.06 ± 0.01	−11.2 ± 1.7	7.8 ± 0.6	2.3 ± 0.3
	LTSL10	133 ± 7	0.06 ± 0.01	−5.6 ± 4.5	6.8 ± 1.3	1.9 ± 0.1
	LTSL15	133 ± 8	0.09 ± 0.04	11.2 ± 3.7	6.7 ± 0.4	2.2 ± 0.4

Table 2
Thermal properties of all the LTSL formulations prepared, determined by DSC: LTSL5 DPPC/MSPC/DSPE-PEG2000 91/5/4 %mol; LTSL10: DPPC/MSPC/DSPE-PEG2000 86/10/4 %mol; LTSL15: DPPC/MSPC/DSPE-PEG2000 81/15/4 %mol. Where indicated, formulations were analyzed in the presence of 10% serum. The samples indicated with asterisk presented two peaks in the thermograms and the calculated values refer to the peak integration of both peaks.

Formulation		Differential scanning calorimetry		
		Onset T, °C	Melting T, °C	Enthalpy, J/g
Control	LTSL5	39.9	40.9	0.955
	LTSL10	40.2	41.5	0.838
	LTSL10 + serum	40.1	41.5	0.935
	LTSL15*	40.5	41.4	0.989
4 kDa dextran	LTSL5	40.0	41.2	1.202
	LTSL10	40.9	41.2	1.087
	LTSL15*	40.1	41.5	1.137
10 kDa dextran	LTSL5	39.9	41.1	1.197
	LTSL10	40.4	41.3	1.073
	LTSL15*	40.1	41.4	1.183
ML1	LTSL5	40.6	40.9	0.957
	LTSL10	40.4	41.4	0.839
	LTSL10 + serum	40.4	41.5	0.838
	LTSL15	40.4	41.0	0.930
BSA	LTSL5	40.6	41.2	1.048
	LTSL10	40.6	41.3	0.837
	LTSL10 + serum	40.7	41.6	0.839
	LTSL15	40.2	41.4	1.018

bilayer, energetically favoring the solid to liquid transition by acting like a membrane defect. Melting enthalpy and T_m were comparable for LTSL10 incubated in buffer or media containing 10% serum. All three formulations with different percentages of MSPC showed similar transition temperature (T_m) of the bilayer (ca 41 °C; T_{onset} 40 °C), although a broader melting track was observed for LTSL with 15% MSPC (Supplementary Fig. SI-3). Incorporation of different mol% of MSPC did not alter the T_m, which remained constant around 41 °C as previously shown [34]. A small side peak was visible in the thermogram for LTSL containing 15% mol MSPC, which is indicative of mismatched phase mixtures caused by two different populations in the composition, as previously reported [34,35].

All three LTSL compositions showed adequate colloidal stability (i.e. particle size and PDI) when stored at 4 °C up to 4 weeks (Fig. 2A–C). Analysis of payload retention, however, showed leakage of the encapsulated cargo with relatively high losses of the payload during storage ((Fig. 2D–G). The most pronounced loss of payloads was observed for the formulations with 5% or 15% MSPC and correlated inversely to the molecular weight (size) of the encapsulated compound, i.e. LTSL loaded with larger macromolecules retained higher percentages of the loaded cargo by the end of the study. It is worth noticing that BSA- and ML1-loaded LTSLs showed comparable profiles and leaked amounts. Since considerable release is observed for all types of macromolecules (dextrans and proteins) it is unlikely that it relates to surface-associated payload that is slowly dissociating from the liposomes. Moreover, the phenomenon is observed for both analytical methods used for determination of payload retention/release (fluorescence detection for FITC-labeled macromolecules and ELISA for ML1 detection). We can only speculate on the mechanism of payload loss, since formation of pores is unlikely at storage conditions below the Tm of LTSL. Our storage stability data indicated that the physicochemical instability of LTSL is related to the lysolipid content, with 10% MSPC affording the best stability. This lipid composition is similar to Thermodox® LTSL formulation and exhibited a superior ML1 retention over the assessed period with approximately 95% ML1 retention after 1 week and 70% after 3 weeks (Fig. 2F, red line).

3.3. Temperature- and time-dependent release kinetics of model macromolecules

To test hyperthermia-triggered release of macromolecular drugs from LTSL, we assessed temperature and time-dependent release of small and medium-sized dextrans, ML1 and albumin, thus covering a wide-range of macromolecular model compounds. Fig. 3 shows the temperature dependent release of model compounds of the tested liposome formulations after a 15-min heating period. LTSL10 showed the preferred release profile for all model compounds. Minor leakage of loaded cargo at 37 °C was observed in all cases. Increasing the temperature to mild hyperthermia, i.e. 42 °C, resulted in up to 46% release of the smallest macromolecular cargo (4 kDa dextran), while approximately 15% of the loaded content was released for the largest model compounds BSA and ML1. LTSL5 and LTSL15 showed a poorer release of all the molecules as compared to LTSL10, indicating that 10% mol MSPC is the optimal MSPC concentration. Fig. 4 shows the time-
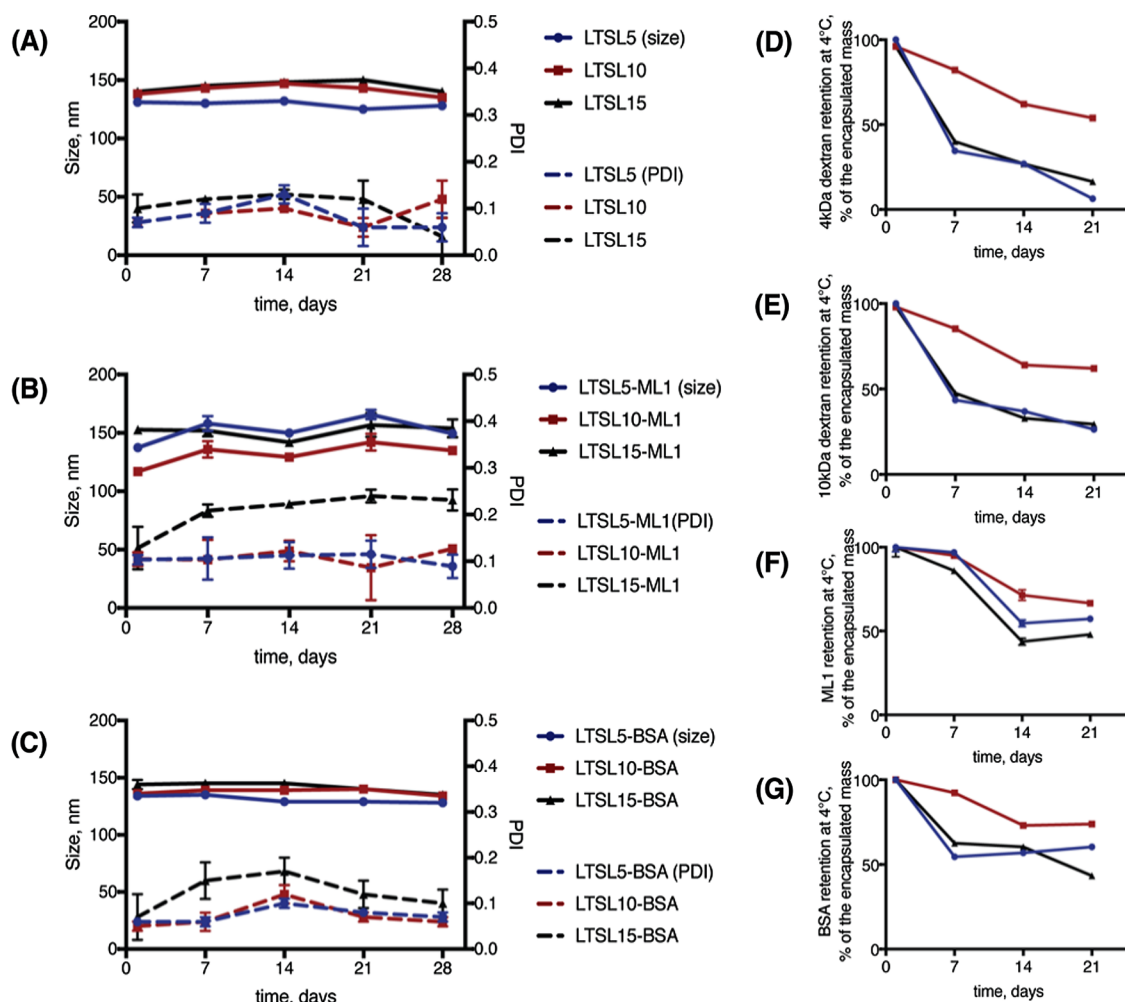
Fig. 2. Storage stability of LTSL at 4 °C in HBS buffer. Left-hand panels show nanoparticles characteristics determined by DLS (continuous lines: size; broken lines: polydispersity); right-hand panels concern retention of loaded cargo in LTSL during storage. (A) control (buffer loaded) LTSL. (B) ML1-loaded LTSL. (C) BSA-loaded LTSL. (D) 4 kDa dextran–loaded LTSL. (E) 10 kDa dextran-loaded LTSL. (F) ML1-loaded LTSL (G) BSA-loaded LTSL. In all graphs, the colors of the lines correspond to the same lipid composition: blue line LTSL5 containing 5%mol MSPC; Red line LTSL10 containing 10 %mol MSPC; Black line LTSL15containing 15 %mol MSPC. Error bars represent average ± standard deviation of 2 independent samples. (For interpretation of the references to colour in this figure legend, the reader is referred to the web version of this article.)

dependent release at 37 °C and 42 °C of all the macromolecules from LTSL10. For all the molecular weight compounds, the release profiles of the LTSL10 exposed to 37 °C revealed minor leakages for during the 30-min period, in contrast with the LTSL10 incubated at 42 °C for the same period of time.

Zhang et al (2011) investigated the heat triggered release of BSA from temperature sensitive liposomes and they demonstrated that approximately 60% of the entrapped BSA can be released within 5 min at 42 °C. The same authors also recovered found that a rather high percentage of the protein is in the bilayer, i.e. aberrantly inserted in the lipid membrane, which could influence the results of release by over quantification [36]. In a recent report [23], the authors also found a size- and time- dependent mechanism for release of macromolecules, including 4 kDa Dextran and FITC-albumin. All these results are in line with the profiles obtained in the present paper: the smaller the entrapped molecule, the more is released from LTSL which suggests that size-restricted membrane passage or diffusion through pores in the bilayer plays a role.

Although the true mechanism behind thermosensitivity in liposomes is still up for debate, it is expected that the transfer (diffusivity) of molecules through the bilayer (from the inner aqueous solution of the liposomes, to the outside) is slower and energetically more unfavorable

than permeation of a very small extremely hydrophilic molecule such as water. This process depends on the partition coefficient (for amphi-philic molecules) and on the size, structure and nature of the solute [37,38]. When defects or pores are created in the liposomes by lysoli-pids, the overall diffusion energy will be lowered, but still the packing defects may be too small to allow free pore diffusion of macromolecules of all size ranges [38].

Overall, our results indicate that, although incomplete, the release obtained from LTSL for macromolecules is most efficient when 10% mol of Lyso-PC is incorporated in the bilayer. We therefore continued the remainder of our studies with this formulation.

3.4. Effect of serum on the release of mistletoe lectin-1

It has been reported that the proteins in the release medium alter the release properties of LTSL formulations in the in vitro and in vivo setups. To investigate this, release studies with ML1 loaded LTSL10 were performed in normothermia and hyperthermia conditions in RPMI culture medium without serum or RPMI culture medium supplemented with 10% serum; the quantification of ML1 release was made by ELISA (Fig. 5). Our results suggest that there is a minor leakage (below 5%) at physiological temperature in the presence of serum. The release at
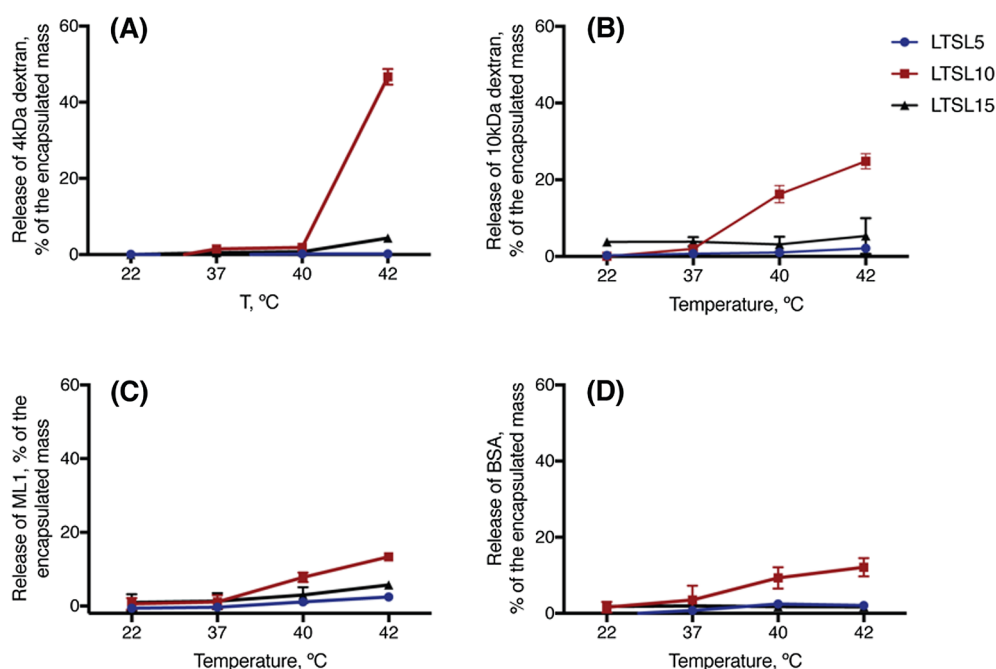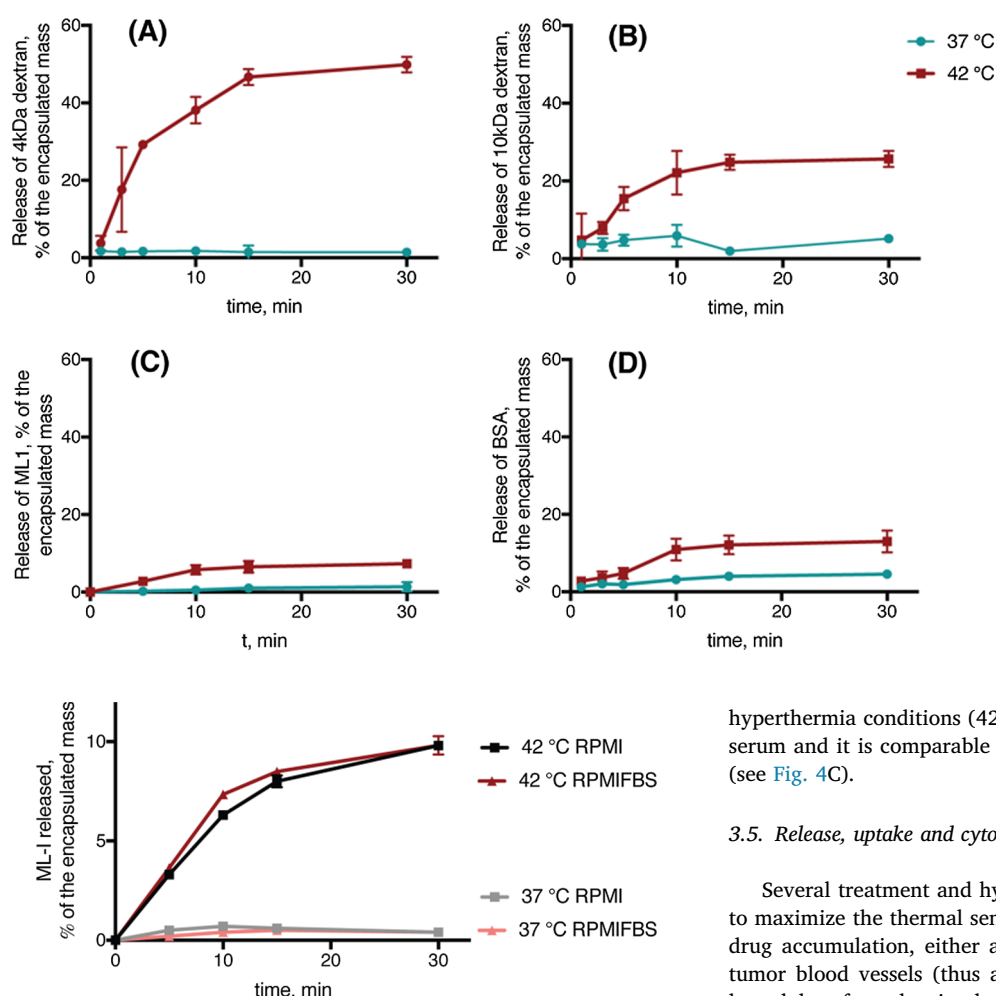
Fig. 3. Hyperthermia triggered release of loaded cargo from LTSL after 15 min incubation at the indicated temperature. (A) LTSL loaded with 4 kDa dextran. (B) LTSL loaded with 10 kDa dextran. (C) LTSL loaded with ML1 (60 kDa). (D) LTSL loaded with BSA (67 kDa). DPPC/MSPC/DSPE-PEG2000 molar ratios: LTSL5 91/5/4 mol% (blue line); LTSL10: 86/10/4 mol% (red line); LTSL15: 81/15/4 mol% (black line). (For interpretation of the references to colour in this figure legend, the reader is referred to the web version of this article.)

Fig. 4. Time-dependent release of loaded cargo from LTSL10 exposed to 37 °C (blue lines) or 42 °C (red lines) for 15 min. (A) LTSL10 loaded with 4 kDa dextran. (B) LTSL10 loaded with 10 kDa dextran. (C) LTSL10 loaded with ML1 (60 kDa). (D) LTSL10 loaded with BSA (67 kDa). (For interpretation of the references to colour in this figure legend, the reader is referred to the web version of this article.)

Fig. 5. Effect of serum in hyperthermia triggered release of ML1 from LTSL10. Black line: LTSL diluted in RPMI (no serum) at 42 °C; dark red line: LTSL diluted in RPMI with 10% serum at 42 °C; grey line: LTSL diluted in RPMI (no serum) at 37 °C; light red line: LTSL diluted in RPMI with 10% serum at 37 °C. (For interpretation of the references to colour in this figure legend, the reader is referred to the web version of this article.)

hyperthermia conditions (42 °C) was not influenced by the presence of serum and it is comparable with the results obtained with HBS buffer (see Fig. 4C).

3.5. Release, uptake and cytotoxicity in tumor cells

Several treatment and hyperthermia protocols have been proposed to maximize the thermal sensitization of cancer cells and intratumoral drug accumulation, either aiming at intravascular release within the tumor blood vessels (thus avoiding EPR and requiring uptake of released drug from the circulation) or intratumoral drug release (i.e. after a lag time allowing accumulation of LTSL within the tumor by EPR). Other heating protocols use a two-step method aiming for more uniform drug distribution throughout the tumor by maximizing tumor perfusion and vascular leakiness in the first step and maximizing drug release in the second step [10,39,40]. The optimal timing between LTSL
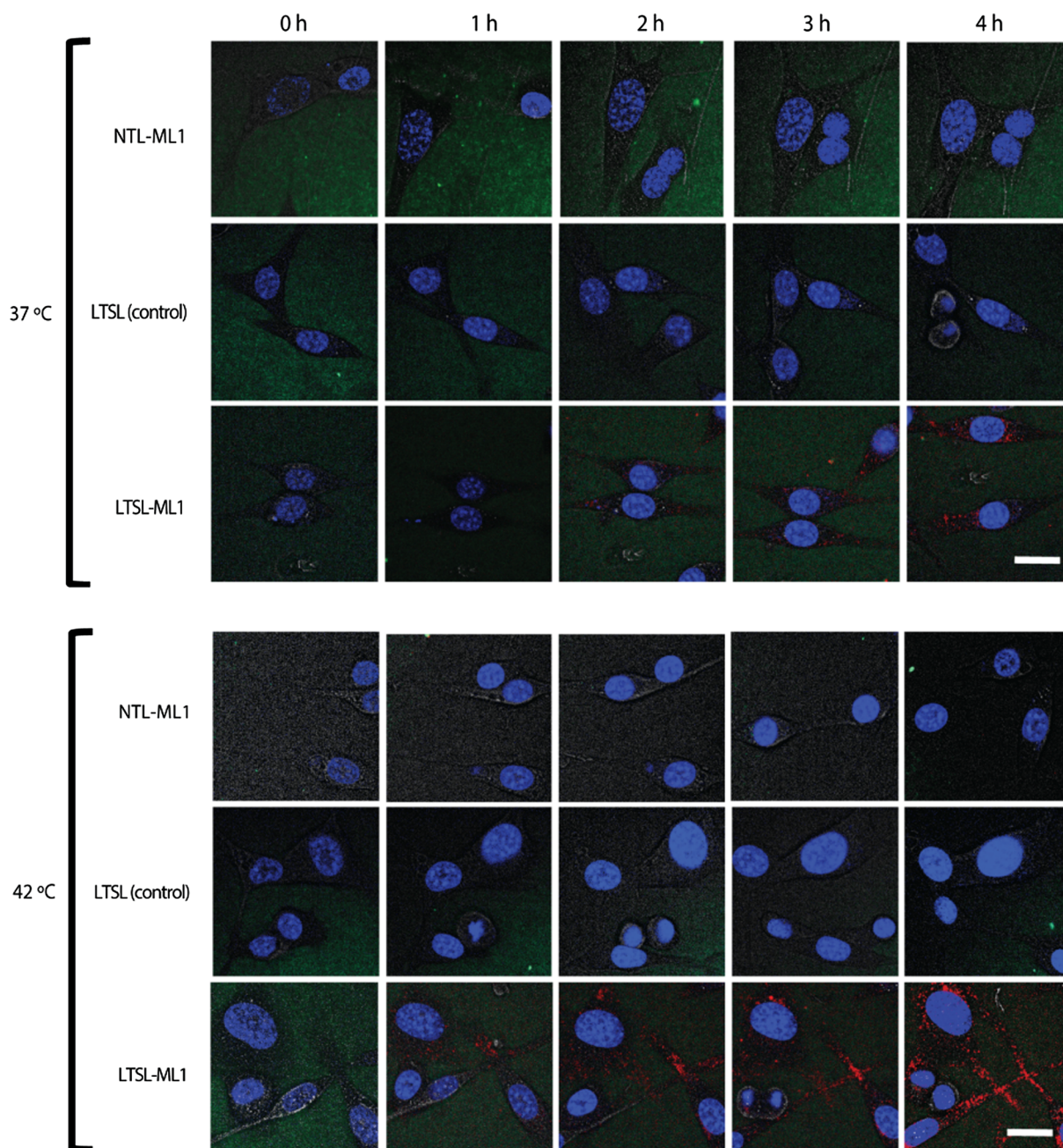
Fig. 6. Uptake of ML1 released from LTSL (setup 1). LTSL were diluted in cell culture media and exposed to mild hyperthermia for 1 h. The resulting media were transferred without further processing onto CT26 and cells were evaluated for 4 h uptake of ML1 by live cell imaging. For the uptake studies, liposomes were labeled with DiO' (green) while ML1 was labeled with AF647 (red). Nuclei of CT26 were stained with Hoechst 33,342 (blue) prior to addition of the preconditioned culture media. Scale bar applies for all live cell images, 20 µm. (For interpretation of the references to colour in this figure legend, the reader is referred to the web version of this article.)

administration and local hyperthermia may depend not only on the tumor physiology, but also on the lipid composition and on the biopharmaceutical properties of the loaded drug, i.e. its capability to enter and stay within the tumor microenvironment. Intravascular release of doxorubicin from LTSL (that is, LTSL administration directly followed by hyperthermia for 30–60 min) proved approximately two-fold more efficacious than intratumoral release (based on EPR accumulation of LTSL, followed by hyperthermia), which was attributed to deeper and more extensive tumor penetration of free doxorubicin as compared to tumor distribution of liposomes [21,41]. Such differences between free doxorubicin and the applied liposomes may largely relate to the efficient uptake of the drug itself and may not be applicable to macromolecules like ML1.

To investigate the overall bioactivity of the formulated ML1 we studied two phenomena related to the two different functional chains of the protein. First, we studied the in vitro uptake in cancer cells by live cell imaging over a time period of 4 h, and we studied ML1 induced cytotoxicity which is only occurring 2 days later (as described before) [31]. ML1 is composed of a cytotoxic A-chain linked to the lectin B-chain responsible for cellular binding and for mediating the protein uptake [42]; thus cytotoxic activity is ensured if the structure of both chains of the protein is conserved. Obviously, uptake and killing of cancer cells should only occur upon hyperthermia treatment of LTSL. In a different setup, we studied the uptake and cytotoxic efficacy when cells were heated together with the LTSL, to observe any bystander effect of the heating procedure.
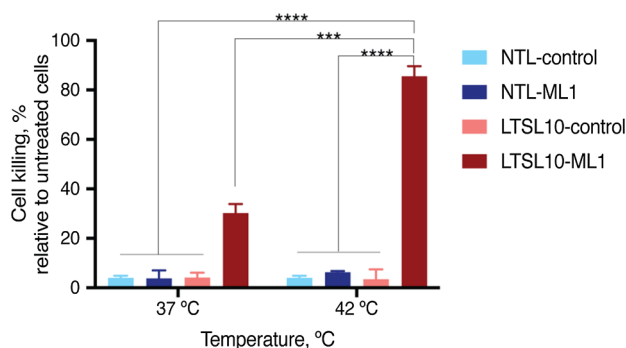
Fig. 7. Bioactivity of ML1 released from LTSL (setup 1). Several concentrations of ML1-loaded LTSL (formulated ML1 10–0.3 µg/mL) were diluted in cell culture media and exposed to mild hyperthermia for 1 h. The resulting media were transferred without further processing onto CT26 After the 4-h uptake period, the cell culture medium was refreshed and cells were cultured for additional 44 h for cytotoxicity (MTS) measurement. Toxicity values represent 48 h cell killing effect of the formulations containing 10 µg/ml of formulated ML1.
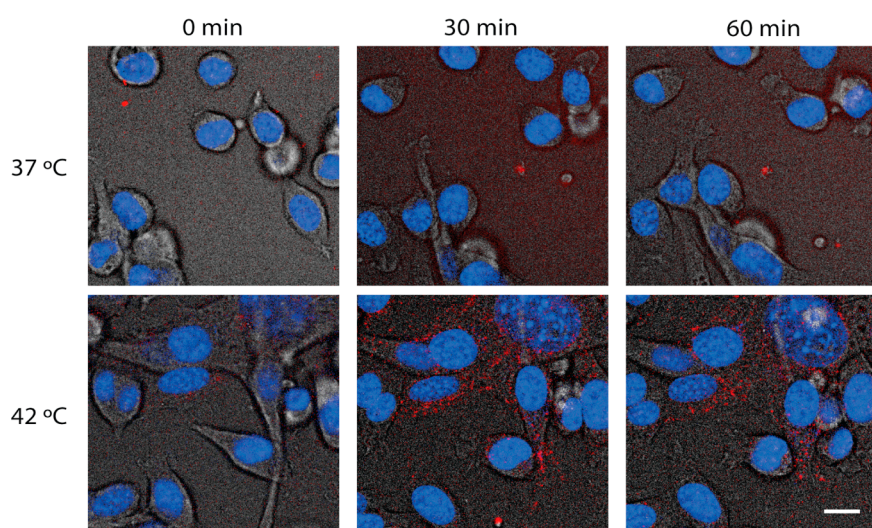
Fig. 6 shows the microscopy pictures of the uptake study. After hyperthermia treatment (42 °C) ML1 released from LTSL was internalized by CT26, resulting in a punctuated red pattern in the cells cytoplasm and leading to potent cytotoxic efficacy after 48 h (IC_{50} = 2.25 µg/mL). As expected, incubating the LTSL10 at 37 °C resulted in a minor release of ML1, and its internalization was less pronounced than at 42 °C. Heating resulted in an 8-fold reduction in IC_{50} (Supplementary Fig. SI-4), which is comparable to the differences in ML1 release between normothermia or hyperthermia conditions (~10-

fold increase in release, see Fig. 5). ML1 formulated in conventional PEG-liposomes was not released and hence showed no uptake (Fig. 6A) nor cytotoxicity (Fig. 7). As expected, buffer loaded LTSL and NTL did not induce cytotoxicity. These results indicate that the lipid formulation used are non-toxic, even at high concentrations. Only LTSL and their combination with hyperthermia results in potent cytotoxic activity of ML1, which thus supports the planned approach of applying localized hyperthermia to the tumor area after administration of ML1-loaded LTSL.
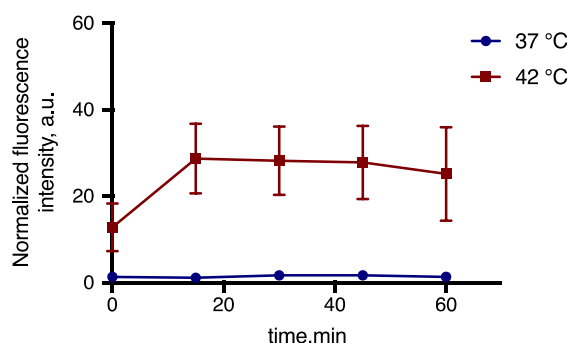
In the second setup, LTSL and cells were heated at 42 °C collectively. As can be observed, the uptake (during an incubation period of 1 h, Fig. 8A and B) and cytotoxicity (after 48 h, Fig. 9A) were strongly enhanced by hyperthermia at 42 °C for 1 h. In the absence of ML1 or liposomes, the control cells exposed at 37 °C or at 42 °C for 1 h (Fig. 9B) showed little differences in terms of cell viability. Thus, these results demonstrate that that the release of the encapsulated toxin can exert potent cytotoxic effects in tumor cells. We therefore conclude that ML1 keeps its bioactivity, which was shown by its cell-binding and uptake, and by tumor cells killing.

4. Conclusions

We have demonstrated the potential of thermosensitive liposomes as nanocarriers for high-molecular weight cytotoxins like ML1. The most suitable liposomal formulation, containing 10 mol% MSPC, complied with all requirements i.e. a homogeneous size, temperature range for hyperthermia and in vitro release tests. Our experiments with CT26 cells confirmed that ML1-LTSL potently inhibited tumor cell viability upon hyperthermia treatment, either after a preheating treatment or

Fig. 8. Release and uptake of ML1 released from LTSL (setup 2). LTSL and CT26 cells were collectively exposed to mild hyperthermia for 1 h and the release and uptake events were evaluated by live cell imaging. (A) For the microscopy studies, ML1 was labeled with AF647 (red). Nuclei of CT26 were stained with Hoechst 33,342 (blue) prior to experiment. Scale bar applies for all live cell images, 20 µm. (B) semi-quantitative analysis of the ML1AF647 cell uptake microscopy studies. Blue line: 37 °C; red line 42 °C. (For interpretation of the references to colour in this figure legend, the reader is referred to the web version of this article.)
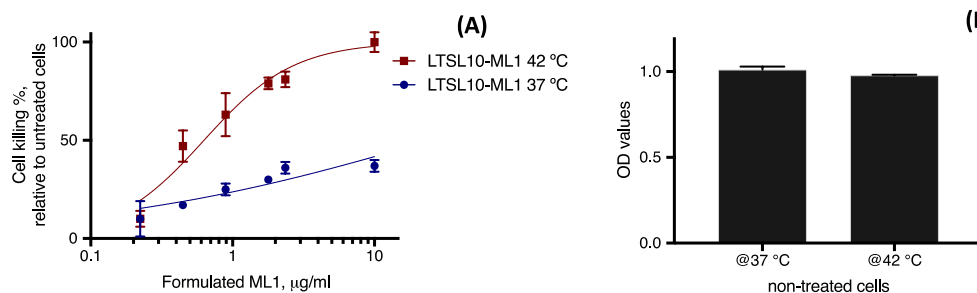
Fig. 9. (A) Bioactivity of ML1 released from LTSL (setup 2). CT26 cells and ML1-loaded LTSL were collectively exposed to mild hyperthermia or normothermic conditions for 1 h; the cell culture medium was refreshed and cells were cultured for additional 47 h for cytotoxicity (MTS) measurement. ML1-loaded LTSL exposed to 42 °C had an IC_{50} of 0.6 µg/ml, while the same formulation exposed to 37 °C had an extrapolated IC_{50} of 25 µg/ml. (B) Effect of heat treatment on CT26 cells, without ML1 or liposomes. Cells were exposed to mild hyperthermia (42 °C) or normothermia (37 °C) conditions for 1 h, and kept for additional 47 h at 37 °C, followed by determination of cell viability by MTS assay. The OD values of the ML1 or liposome treated samples in (A) were normalized to the correspondent negative control OD value in (B).

when cells were coincubated with ML1-LTSL. These promising results warrant further investigation of the developed thermosensitive formulation of ribosome-inactivating cytotoxins.

Acknowledgments

Appendix A. Supplementary material

Supplementary data to this article can be found online at https://doi.org/10.1016/j.ejpb.2018.09.010.

References

[1] Y. Matsumura, H. Maeda, A new concept for macromolecular therapeutics in cnacer chemotherapy: mechanism of tumoritropic accumulatio of proteins and the anti-tumor agents Smancs, Cancer Res. 46 (1986) 6387–6392, https://doi.org/10.1021/bc100070g.

[2] E. Oude Blenke, E. Mastrobattista, R.M. Schiffelers, Strategies for triggered drug release from tumor targeted liposomes, Expert Opin. Drug Deliv. 10 (2013) 1399–1410, https://doi.org/10.1517/17425247.2013.805742.

[3] A. Wicki, D. Witzigmann, V. Balasubramanian, J. Huwyler, Nanomedicine in cancer therapy: challenges, opportunities, and clinical applications, J. Control. Release 200 (2015) 138–157, https://doi.org/10.1016/j.jconrel.2014.12.030.

[4] M. Karimi, A. Ghasemi, P. Sahandi Zangabad, R. Rahighi, S.M. Moosavi Basri, H. Mirshekari, M. Amiri, Z. Shafaei Pishabad, A. Aslani, M. Bozorgomid, D. Ghosh, A. Beyzavi, A. Vaseghi, A.R. Aref, L. Haghani, S. Bahrami, M.R. Hamblin, Smart micro/nanoparticles in stimulus-responsive drug/gene delivery systems, Royal Soc. Chem. (2016), https://doi.org/10.1039/C5CS00798D.

[5] C. Alvarez-Lorenzo, A. Concheiro, Smart drug delivery systems: from fundamentals to the clinic, Chem. Commun. (Camb.) 50 (2014) 7743–7765, https://doi.org/10.1039/c4cc01429d.

[6] S. Mura, J. Nicolas, P. Couvreur, Stimuli-responsive nanocarriers for drug delivery, Nat. Mater. 12 (2013) 991–1003, https://doi.org/10.1038/nmat3776.

[7] Z. Al-Ahmady, K. Kostarelos, Chemical components for the design of temperature-responsive vesicles as cancer therapeutics, Chem. Rev. 116 (2016) 3883–3918, https://doi.org/10.1021/acs.chemrev.5b00578.

[8] L. Li, T.L.M. ten Hagen, D. Schipper, T.M. Wijnberg, G.C. van Rhoon, A.M.M. Eggermont, L.H. Lindner, G.A. Koning, Triggered content release from optimized stealth thermosensitive liposomes using mild hyperthermia, J. Control. Release 143 (2010) 274–279, https://doi.org/10.1016/j.jconrel.2010.01.006.

[9] S.M. Park, M.S. Kim, S.J. Park, E.S. Park, K.S. Choi, Y.S. Kim, H.R. Kim, Novel temperature-triggered liposome with high stability: Formulation, in vitro evaluation, and in vivo study combined with high-intensity focused ultrasound (HIFU), J. Control. Release 170 (2013) 373–379, https://doi.org/10.1016/j.jconrel.2013.06.003.

[10] L. Li, T.L.M. Ten Hagen, M. Bolkestein, A. Gasselhuber, J. Yatvin, G.C. Van Rhoon, A.M.M. Eggermont, D. Haemmerich, G.A. Koning, Improved intratumoral nano-particle extravasation and penetration by mild hyperthermia, J. Control. Release 167 (2013) 130–137, https://doi.org/10.1016/j.jconrel.2013.01.026.

[11] B.M. Dicheva, G.A. Koning, Targeted thermosensitive liposomes: an attractive novel approach for increased drug delivery to solid tumors, Expert Opin. Drug Deliv. 11 (2014) 83–100, https://doi.org/10.1517/17425247.2014.866650.

[12] T. Ta, T.M. Porter, Thermosensitive liposomes for localized delivery and triggered release of chemotherapy, J. Control. Release 169 (2013) 112–125, https://doi.org/10.1016/j.jconrel.2013.03.036.

[13] D. Chen, W. Liu, Y. Shen, H. Mu, Y. Zhang, R. Liang, A. Wang, K. Sun, F. Fu, Effects of a novel pH-sensitive liposome with cleavable esterase-catalyzed and pH-responsive double smart mPEG lipid derivative on ABC phenomenon, Int. J. Nanomed. 6 (2011) 2053–2061, https://doi.org/10.2147/IJN.S24344.

[14] Y. Dou, K. Hynynen, C. Allen, To heat or not to heat: challenges with clinical translation of thermosensitive liposomes, J. Control. Release 249 (2017) 63–73, https://doi.org/10.1016/j.jconrel.2017.01.025.

[15] W.J.M. Lokerse, E.C.M. Kneepkens, T.L.M. ten Hagen, A.M.M. Eggermont, H. Grüll, G.A. Koning, In depth study on thermosensitive liposomes: optimizing formulations for tumor specific therapy and in vitro to in vivo relations, Biomaterials 82 (2016) 138–150, https://doi.org/10.1016/j.biomaterials.2015.12.023.

[16] B.M. Dicheva, T.L.M. Ten Hagen, D. Schipper, A.L.B. Seynhaeve, G.C. Van Rhoon, A.M.M. Eggermont, G.A. Koning, Targeted and heat-triggered doxorubicin delivery to tumors by dual targeted cationic thermosensitive liposomes, J. Control. Release 195 (2014) 37–48, https://doi.org/10.1016/j.jconrel.2014.07.058.

[17] B.M. Dicheva, T.L.M. Ten Hagen, L. Li, D. Schipper, A.L.B. Seynhaeve, G.C. Van Rhoon, A.M.M. Eggermont, L.H. Lindner, G.A. Koning, Cationic thermosensitive liposomes: a novel dual targeted heat-triggered drug delivery approach for endothelial and tumor cells, Nano Lett. 13 (2013) 2324–2331, https://doi.org/10.1021/nl3014154.

[18] L. Li, T.L.M. TenHagen, M. Hossann, R. Süss, G.C. VanRhoon, A.M.M. Eggermont, D. Haemmerich, G.A. Koning, Mild hyperthermia triggered doxorubicin release from optimized stealth thermosensitive liposomes improves intratumoral drug delivery and efficacy, J. Control. Release 168 (2013) 142–150, https://doi.org/10.1016/j.jconrel.2013.03.011.

[19] G.A. Koning, A.M.M. Eggermont, L.H. Lindner, T.L.M. ten Hagen, Hyperthermia and thermosensitive liposomes for improved delivery of chemotherapeutic drugs to solid tumors, Pharm. Res. 27 (2010) 1750–1754, https://doi.org/10.1007/s11095-010-0154-2.

[20] D.K. Chang, C.Y. Chiu, S.Y. Kuo, W.C. Lin, A. Lo, Y.P. Wang, P.C. Li, H.C. Wu, Antiangiogenic targeting liposomes increase therapeutic efficacy for solid tumors, J. Biol. Chem. 284 (2009) 12905–12916, https://doi.org/10.1074/jbc.M900280200.

[21] C.D. Landon, J.-Y. Park, D. Needham, M.W. Dewhirst, Nanoscale drug delivery and hyperthermia: the materials design and preclinical and clinical testing of low temperature- sensitive liposomes used in combination with mild hyperthermia in the treatment of local cancer, Open Nanomed. J. 3 (2011) 38–64, https://doi.org/10.2174/1875933501103010038.Nanoscale.

[22] V. Saxena, C. Gacchina Johnson, A.H. Negussie, K.V. Sharma, M.R. Dreher, B.J. Wood, Temperature-sensitive liposome-mediated delivery of thrombolytic agents, Int. J. Hyperth. 31 (2015) 67–73, https://doi.org/10.3109/02656736.2014.991428.

[23] X. Huang, M. Li, R. Bruni, P. Messa, F. Cellesi, The effect of thermosensitive liposomal formulations on loading and release of high molecular weight biomolecules, Int. J. Pharm. 524 (2017) 279–289, https://doi.org/10.1016/j.ijpharm.2017.03.090.

[24] M. Marvibaigi, E. Supriyanto, N. Amini, F.A. Abdul Majid, S.K. Jaganathan, Preclinical and clinical effects of mistletoe against breast cancer, Biomed Res. Int. 2014 (2014) 785479, https://doi.org/10.1155/2014/785479.

[25] M. Horneber, G. Bueschel, R. Huber, K. Linde, M. Rostock, M. Horneber, G. Bueschel, R. Huber, K. Linde, M. Rostock, Mistletoe therapy in oncology (Review), Cochrane Libr. (2010) 4–6, https://doi.org/10.1002/14651858.CD003297.pub2.Copyright.

[26] M. Puri, F. Kaur, M.A. Perugini, R.C. Gupta, Ribosome-inactivating proteins: Current status and biomedical applications, Drug Discov. Today. 17 (2012) 774–783, https://doi.org/10.1016/j.drudis.2012.03.007.

[27] F. Stirpe, Ribosome-inactivating proteins: From toxins to useful proteins, Toxicon 67 (2013) 12–16, https://doi.org/10.1016/j.toxicon.2013.02.005.

[28] G. Ribéreau-Gayon, S. Dumont, C. Muller, M.L. Jung, P. Poindron, R. Anton, Mistletoe lectins I, II and III induce the production of cytokines by cultured human monocytes, Cancer Lett. 109 (1996) 33–38, https://doi.org/10.1016/S0304-3835(96)04401-1.

[29] A. Thies, D. Nugel, U. Pfüller, I. Moll, U. Schumacher, Influence of mistletoe lectins and cytokines induced by them on cell proliferation of human melanoma cells in vitro, Toxicology 207 (2005) 105–116, https://doi.org/10.1016/j.tox.2004.09.009.

[30] A. Thies, P. Dautel, A. Meyer, U. Pfüller, U. Schumacher, Low-dose mistletoe lectin-I

reduces melanoma growth and spread in a scid mouse xenograft model, Br. J. Cancer 98 (2008) 106–112, https://doi.org/10.1038/sj.bjc.6604106.

[31] N. Beztsinna, M.B.C. de Matos, J. Walther, C. Heyder, E. Hildebrandt, G. Leneweit, E. Mastrobattista, R.J. Kok, Quantitative analysis of receptor-mediated uptake and pro-apoptotic activity of mistletoe lectin-1 by high content imaging, Sci. Rep. 8 (2018) 2768, https://doi.org/10.1038/s41598-018-20915-y.

[32] R. Eifler, K. Pfuller, W. Gockeritz, U. Pfuller, Improved procedures for isolation of mistletoe lectins and their subunits: lectin pattern of the European Mistletoe, in: J. Basu, M. Kundu, P. Chakrabari, T. Bog-Hansen (Eds.), Lectins 9 Biol. Biochem. Clin. Biochem. 9th ed., Wiley Eastern Limited, New Delhi, 1993, pp. 1–5.

[33] G. Rouser, S. Fleischer, A. Yamamoto, Two dimensional thin layer chromatographic separation of polar lipids and determination of phospholipids by phosphorus analysis of spots, Lipids 5 (1970) 494–496, https://doi.org/10.1007/BF02531316.

[34] J.K. Mills, D. Needham, Lysolipid incorporation in dipalmitoylphosphatidylcholine bilayer membranes enhances the ion permeability and drug release rates at the membrane phase transition, Biochim. Biophys. Acta - Biomembr. 1716 (2005) 77–96, https://doi.org/10.1016/j.bbamem.2005.08.007.

[35] D. Needham, M.W. Dewhirst, The development and testing of a new temperature-sensitive drug delivery system for the treatment of solid tumors, Adv. Drug Deliv. Rev. 53 (2001) 285–305, https://doi.org/10.1016/S0169-409X(01)00233-2.

[36] X. Zhang, P.F. Luckham, A.D. Hughes, S. Thom, X.Y. Xu, Development of lysolipid-based thermosensitive liposomes for delivery of high molecular weight proteins, Int. J. Pharm. 421 (2011) 291–292, https://doi.org/10.1016/j.ijpharm.2011.09.016.

[37] M. Hossann, T. Wang, M. Wiggenhorn, R. Schmidt, A. Zengerle, G. Winter, H. Eibl, M. Peller, M. Reiser, R.D. Issels, L.H. Lindner, Size of thermosensitive liposomes influences content release, J. Control. Release 147 (2010) 436–443, https://doi.org/10.1016/j.jconrel.2010.08.013.

[38] T.-X. Xiang, B.D. Anderson, Liposomal drug transport: a molecular perspective from molecular dynamics simulations in lipid bilayers, Adv. Drug Deliv. Rev. 58 (2006) 1357–1378, https://doi.org/10.1016/j.addr.2006.09.002.

[39] A.M. Ponce, B.L. Viglianti, D. Yu, P.S. Yarmolenko, C.R. Michelich, J. Woo, M.B. Bally, M.W. Dewhirst, Magnetic resonance imaging of temperature-sensitive liposome release: drug dose painting and antitumor effects, JNCI J. Natl. Cancer Instit. 99 (2007) 53–63, https://doi.org/10.1093/jnci/djk005.

[40] L. Li, T.L.M. Ten Hagen, A. Haeri, T. Soullié, C. Scholten, A.L.B. Seynhaeve, A.M.M. Eggermont, G.A. Koning, A novel two-step mild hyperthermia for advanced liposomal chemotherapy, J. Control. Release 174 (2014) 202–208, https://doi.org/10.1016/j.jconrel.2013.11.012.

[41] A.A. Manzoor, L.H. Lindner, C.D. Landon, J. Park, A.J. Simnick, M.R. Dreher, S. Das, G. Hanna, W. Park, A. Chilkoti, G.A. Koning, T.L.M. Hagen, D. Needham, M.W. Dewhirst, Overcoming limitations in nanoparticle drug delivery: triggered, Intravascular Release Improve Drug Penetration Tumors 72 (2012) 5566–5576, https://doi.org/10.1158/0008-5472.CAN-12-1683.

[42] E. Pizzo, A. Di Maro, A new age for biomedical applications of Ribosome Inactivating Proteins (RIPs): from bioconjugate to nanoconstructs, J. Biomed. Sci. 23 (2016) 54, https://doi.org/10.1186/s12929-016-0272-1.